Mathematical Modelling of Lung Cancer Growth with Innate Immune Cell Response and The Role of Mesenchymal Stem Cell

Ilham K.* and Lina Aryati

***Abstract*—Lung cancer is a leading cause of cancer-related mortality worldwide. A comprehensive understanding of the dynamics of lung cancer growth and its interactions with the immune system is crucial for the development of effective treatments. This study aims to model and analyze lung cancer growth by considering the response of innate immune cells and the role of mesenchymal stem cells (MSCs). A mathematical model is developed to describe the interactions between lung cancer cells, $CD8^+$ T cells, dendritic cells, and MSCs. The model employs nonlinear differential equations to represent the growth dynamics of these cells and the factors influencing them, such as proliferation rates, activation, and inhibition. Subsequently, a mathematical analysis of the model is conducted, including stability analysis, sensitivity analysis, and numerical simulations. Stability analysis is used to identify the stable cancer-free equilibrium points, while sensitivity analysis determines the parameters that significantly affect lung cancer growth. Numerical simulations are performed to validate the results of the mathematical analysis. The findings of this study demonstrate that the mathematical model accurately represents the dynamics of lung cancer growth, including the response of $CD8^+$ T cells, dendritic cells, and MSCs. Furthermore, the results highlight that dendritic cells play a critical role in inhibiting lung cancer growth, whereas the presence of MSCs accelerates the metastasis of lung cancer cells.**

***Index Terms*—Lung cancer, CD8+ T, Dendritic cell, Mesenchymal Stem Cell, Mathematical modelling.**

I. Introduction

LUNG cancer is one of the leading causes of cancer-related deaths worldwide [1]. Lung cancer consists of two main types: non-small cell lung cancer (NSCLC) and small cell lung cancer (SCLC) where NSCLC, as the most common type of lung cancer [2], accounts for 85% of all lung cancer cases. According to Jain [3], NSCLC is divided into three categories: Adenocarcinoma, Squamous-cell carcinoma, and Large-cell carcinoma. The overall 5-year survival rate for patients with lung cancer is less than 15%, and for patients with clinically diagnosed stage IV NSCLC, it is less than 5% [4]. The main cause of lung cancer is smoking, which involves around 93 carcinogens harmful to human health, including nicotine, nitrosamines, and benzene [5]. One of these carcinogens, polycyclic aromatic hydrocarbon benzo[a]pyrene (B[a]P), increases the secretion of osteopontin (OPN) from lung cancer cells through the JAK2/STAT3 signaling pathway. High levels of OPN in the lung tumor microenvironment (TME) stimulate mesenchymal stem cells (MSCs) to infiltrate and adhere to cancer cells, thereby promoting tumor growth [6]. Mesenchymal Stem Cells (MSCs) are a type of multipotent cell with the ability to differentiate and self-renew. When properly stimulated, MSCs can differentiate into various cell types (such as fibroblasts, adipocytes, chondrocytes, and osteoblasts) and perform various roles [7]. However, MSCs also experience a decline in function, partly due to cellular aging, which inhibits their differentiation and proliferation [8]. The primary source of MSCs is believed to be bone marrow (BM), although their presence is minimal, only 0.001-0.01% of the total nucleated cells [9]. MSCs can also be effectively extracted from other tissues, such as the umbilical cord [1], umbilical cord blood [10], amniotic membrane [11], placenta [12], peripheral blood [13], muscle [14], and lungs [15]. MSCs derived from both lung cancer tissue and normal lung tissue accelerate lung cancer metastasis [16]. Additionally, MSCs suppress the activation of immune cells such as dendritic cells (DCs) and T cells, thereby further accelerating cancer cell growth [17]. Dendritic cells (DCs) are professional antigen-presenting immune cells that process and present antigens through major histocompatibility complex molecules I and II (MHC I and II) to the innate and adaptive immune systems [18]. DCs originate from the bone marrow, then circulate through the blood and enter lymphoid glands to function as lymphoid DCs or enter peripheral tissues to differentiate into non-lymphoid DCs [19]. DCs are derived from lymphoid and myeloid lineages in the bone marrow, which produce conventional DCs (cDCs) and plasmacytoid DCs (pDCs), respectively [20]. Based on their development, DCs are categorized into mature and immature cells [21].

The mechanism of DCs as antigen presenters involves identifying and engulfing pathogens before presenting them to immune cells like T cells. This process involves interactions between surface receptors and co-stimulatory proteins that activate the immune response. Subsequently, DCs release cytokines and chemokines that can influence the microenvironment and tumor formation [22]. Exosomes produced by lung tumor cells efficiently transport various tumor antigens to DCs, as well as signaling molecules, facilitating intercellular contact [23]. Antigens carried by exosomes associated with lung cancer have been shown to stimulate DC maturation and cross-presentation of MHC, resulting in specific cytotoxic T cell responses against the tumor [24]. In addition to presenting antigens and activating T cells, DCs can also directly kill cancer cells [25]. One of the T cells activated by DCs is the CD8+ T cell. Cytotoxic

Manuscript received September 5, 2024; revised May 27, 2025

*Ilham K. is a postgraduate student at the Department of Mathematics, Faculty of Mathematics and Natural Sciences, Universitas Gadjah Mada, Yogyakarta, Indonesia (Corresponding author to provide. e-mail: ilhamkandari62@gmail.com, ilhamk@mail.ugm.ac.id)

Lina Aryati is a Lecturer at the Department of Mathematics, Faculty of Mathematics and Natural Sciences, Universitas Gadjah Mada, Yogyakarta, Indonesia (e-mail: lina@ugm.ac.id)

CD8+ T cells from the adaptive immune system are the most effective effectors in the anti-cancer immune response [26]. CD8+ T cells play a central role in mediating anti-tumor immunity and eliminating tumor cells by recognizing tumor-associated antigens present in major histocompatibility complex class I [27]. There is substantial evidence of the effect of CD8+ T cell infiltration on tumor prognosis [28]. Research indicates that CD8+ T cell infiltration is correlated with a better prognosis in lung cancer [29]. Mathematical modeling of lung cancer cell growth has been conducted by several researchers. Among them, the study by Ullah [30] models lung cancer cell growth by involving immune cells such as dendritic cells and CD8+ T cells. Furthermore, the study by Efti [31] discusses lung cancer cell growth by involving macrophage cells. However, mathematical modeling that involves MSCs is still rare or even nonexistent. Based on research conducted by Jiang [6], MSCs play a very important role in the growth of lung cancer cells. Therefore, this thesis will discuss the formation of a mathematical model of lung cancer cell growth that involves dendritic cells, CD8+ T cells, and MSCs.

II. Model Formulation

The formulation of this mathematical model is used to describe the interactions between lung cancer cells, CD8+ T cells, dendritic cells, and mesenchymal stem cells (MSCs). Based on the medical explanation in the previous subsection, let $L(t)$ denote the concentration of lung cancer cells at time t, $C(t)$ denote the concentration of adaptive immune CD8+ T cells at time t, $D(t)$ denote the concentration of dendritic cells at time t, and $M(t)$ denote the concentration of MSCs at time t. For convenience, $L(t)$, $C(t)$, $D(t)$, and $M(t)$ will hereafter be referred to simply as L, C, D, and M, respectively.

1) Modeling The Dynamic of Lung Cancer Cells: The growth of cancer is assumed to follow a logistic growth model, where α and K_l represent the growth rate and carrying capacity of lung cancer cells, respectively. Additionally, β denotes the interaction coefficient between cancer cells and MSCs, which is influenced by cigarette smoke. Cigarette smoke increases the expression of osteopontin (OPN), thereby accelerating the recruitment of MSCs into lung cancer cells and promoting metastasis. Lung cancer cells are also subject to reduction due to interactions with immune cells, specifically CD8+ T cells, with a death rate of γ. The interaction between dendritic cells and cancer cells can further contribute to the reduction of cancer cells, with a death rate of σ. The dynamics of tumor cells are described by the following ordinary differential equation:

$$\frac{dL}{dt} = \alpha L\left(1 - \frac{L}{K_l}\right) + \beta ML - \gamma LC - \sigma LD$$

2) Modeling The Dynamic of CD8+ T: The interaction between lung cancer cells and dendritic cells activates CD8+ T cells at an activation rate of δ. Additionally, lung cancer cells can inhibit CD8+ T cells as a form of self-defense at a rate of φ. It is also known that the presence of MSCs further inhibits CD8+ T cells. Moreover, μ represents the natural death rate of CD8+ T cells. The dynamics of CD8+ T cells can be described by the following ordinary differential equation:

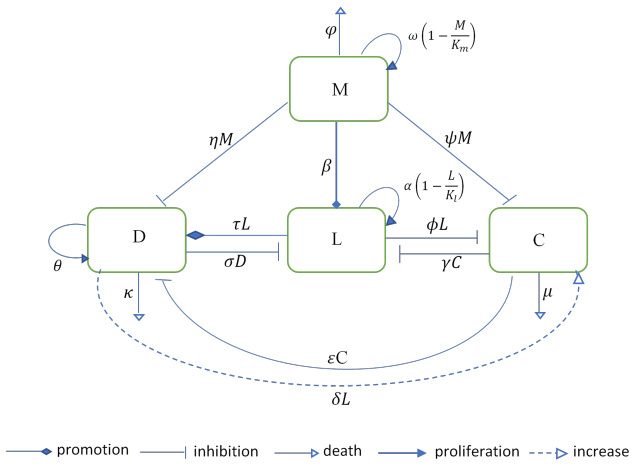

Fig. 1. Flow Chart of Lung Cancer Cell Growth Dynamics

equation:

$$\frac{dC}{dt} = \delta LD - \phi LC - \psi MC - \mu C$$

3) Modeling The Dynamic of Dendritic Cells: The constant θ represents the constant recruitment of dendritic cells from other sources. The interaction between cancer cells and dendritic cells leads to the maturation of dendritic cells at a rate of τ. Additionally, some dendritic cells can be deactivated by CD8+ T cells with a deactivation coefficient of ε. The maturation of dendritic cells can also be inhibited due to interactions with mesenchymal stem cells (MSCs), represented by the coefficient η. Furthermore, κ represents the natural death rate of dendritic cells. The dynamics of dendritic cells can be described by the following ordinary differential equation:

$$\frac{dD}{dt} = \theta + \tau LD - \varepsilon CD - \eta MD - \kappa D$$

4) Modeling The Dynamic of MSCs: The dynamics of MSCs growth are modeled using a logistic function, with ω representing the natural growth rate of MSCs and K_m denoting the carrying capacity. Additionally, φ represents the coefficient for the natural death rate of MSCs. The dynamics of MSCs can be described by the following ordinary differential equation:

$$\frac{dM}{dt} = \omega M\left(1 - \frac{M}{K_m}\right) - \varphi M$$

Based on the description above, the system of nonlinear differential equations governing the dynamics of lung cancer cell growth is given by the following equations. See also Figure 1.

$$\begin{cases} \frac{dL}{dt} = & \alpha L\left(1 - \frac{L}{K_l}\right) + \beta ML - \gamma LC - \sigma LD \\ \frac{dC}{dt} = & \delta LD - \phi LC - \psi MC - \mu C \\ \frac{dD}{dt} = & \theta + \tau LD - \varepsilon CD - \eta MD - \kappa D \\ \frac{dM}{dt} = & \omega M\left(1 - \frac{M}{K_m}\right) - \varphi M \end{cases} \tag{1}$$

III. Properties Of Solution

***Lemma** 3.1:* Suppose $L(0) \geq 0$, $C(0) \geq 0$, $D(0) > 0$, and $M(0) > 0$, then $L(t) \geq 0$, $C(t) \geq 0$, $D(t) > 0$, and $M(t) > 0$ for all $t \in [0, T]$ where $T > 0$.

Proof: It is important to note that all parameters used in System (1) are positive. We now proceed to prove that $L(t)$, $C(t)$, $D(t)$, and $M(t)$ remain positive for every $t \in [0, T]$ in R_+^4. Based on the first equation in System (1), we obtain:

$$\begin{aligned}
&\frac{dL}{dt} = L\left(\alpha - \frac{\alpha L}{K_l} + \beta M - \gamma C - \sigma D\right) \\
\Leftrightarrow &\int_0^t \frac{dL}{L} = \int_0^t \left(\alpha - \frac{\alpha L}{K_l} + \beta M - \gamma C - \sigma D\right) dt \\
\Leftrightarrow \quad &L(t) = L(0) e^{\int_0^t \left(\alpha - \frac{\alpha L}{K_l} + \beta M - \gamma C - \sigma D\right) dt} \geq 0.
\end{aligned}$$

Therefore, we have $L(t) \geq 0$.
Then, based on the second equation in System (1), and assuming $A_1 = \tau L - \varepsilon C - \eta M - \kappa$, we obtain:

$$\begin{aligned}
&\frac{dD}{dt} - A_1 D = \theta \\
\Rightarrow &\int_0^t d\left(e^{\int -A_1 dt} D\right) = \int_0^t \theta e^{\int -A_1 dt} dt > 0 \\
\Rightarrow &\int_0^t d\left(e^{\int -A_1 dt} D\right) > 0.
\end{aligned}$$

Suppose $H_1(t) = \int -A_1 \, dt$, then we obtain

$$D(t) > e^{H_1(0)} D(0) e^{-H_1(t)} > 0,$$

Therefore, we have $D(t) > 0$.
Then, based on the third equation in System (1), and assuming $A_2 = (\phi L + \psi M + \mu)$, we obtain

$$\begin{aligned}
&\frac{dC}{dt} + A_2 C = \delta L D \\
\Leftrightarrow &d\left(e^{\int A_2 dt} C\right) = \delta L D e^{\int A_2 dt} dt \\
\Rightarrow &\int_0^t d\left(e^{\int A_2 dt} C\right) = \int_0^t \delta L D e^{\int A_2 dt} dt.
\end{aligned}$$

Since $L \geq 0$ and $D > 0$, we obtain

$$\begin{aligned}
&\int_0^t d\left(e^{\int A_2 dt} C\right) = \int_0^t \delta L D e^{\int A_2 dt} dt \geq 0 \\
\Leftrightarrow &\int_0^t d\left(e^{\int A_2 dt} C\right) \geq 0.
\end{aligned}$$

Suppose $H_2(t) = \int A_2 \, dt$, then we obtain

$$C(t) \geq e^{H_2(0)} C(0) e^{-H_2(t)} \geq 0,$$

Therefore, we have $C(t) \geq 0$.
Based on the fourth equation in System (1), we obtain

$$\begin{aligned}
&\frac{dM}{M} = \left(\omega - \frac{\omega M}{K_m} - \varphi\right) dt \\
\Rightarrow &M(t) = M(0) e^{\int_0^t \left(\omega - \frac{\omega M}{K_m} - \varphi\right) dt} > 0,
\end{aligned}$$

Therefore, we have $M(t) > 0$.
Next, we define the feasible region Ω as follows:

$$\Omega = \left\{(L(t), C(t), D(t), M(t) \in R_+^4 | N(t) \leq \bar{c}\right\},$$

where

$$\begin{aligned}
N(t) &= L(t) + C(t) + D(t) + M(t) \\
\bar{c} &= \frac{K}{\varphi} + \frac{c_6}{\mu} + \frac{c_5}{\kappa} + c_2 K_m \\
c_1 &= \omega - \varphi \\
c_2 &= \frac{c_1}{\omega} \\
c_4 &= \alpha + \beta c_2 K_m + \varphi \\
c_5 &= \frac{\alpha K}{\varphi} + \frac{\beta c_2 K_m K}{\varphi} + \theta + \frac{\kappa K}{\varphi} \\
c_6 &= \frac{\delta c_5 K}{\varphi \kappa} \\
K &= \frac{c_4^2 K_l}{4\alpha} + \frac{\omega K_m}{4}.
\end{aligned}$$

***Theorem** 3.2:* If $\omega > \varphi$ and $\sigma > \tau$, then the feasible region Ω is a positively invariant and bounded set for System (1).

Proof: It is important to note that, from the fourth equation in System (1), we obtain:

$$\frac{dM}{dt} = \omega M \left(\frac{c_1}{\omega} - \frac{M}{K_m}\right). \tag{2}$$

Since $c_2 = \frac{c_1}{\omega}$, Equation (2) becomes

$$\begin{aligned}
&\frac{dM}{dt} = \omega M \left(c_2 - \frac{M}{K_m}\right) \\
\Rightarrow &M(t) = \frac{M(0)}{c_2 K_m - M(0)} e^{c_2 \omega t} \left[c_2 K_m - M(t)\right]. \qquad (3)
\end{aligned}$$

Suppose $c_3 = \frac{M(0)}{c_2 K_m - M(0)}$, then the solution to Equation (3) is obtained as follows

$$\begin{aligned}
M(t) &= \frac{c_2 K_m}{\frac{1}{c_3} e^{-c_2 \omega t} + 1} \\
&\Rightarrow M \leq c_2 K_m \qquad (4)
\end{aligned}$$

Next, we prove that L is bounded. To demonstrate this, we define the following function

$$P_1 = L + M.$$

Based on Lemma 3.1, L, C, D, and M are positive, and it is known that $M(t) \leq c_2 K_m$. Therefore, we obtain:

$$\begin{aligned}
\frac{dP_1}{dt} =& \frac{dL}{dt} + \frac{dM}{dt} \\
\leq& \alpha L - \frac{\alpha L^2}{K_l} + \beta c_2 K_m L + \omega M - \frac{\omega M^2}{K_m} - \varphi M \\
\frac{dP_1}{dt} + \varphi P_1 \leq& - \frac{\alpha L^2}{K_l} - \frac{\omega M^2}{K_m} + c_4 L + \omega M, \qquad (5)
\end{aligned}$$

where $c_4 = \alpha + \beta c_2 K_m + \varphi$. Then, we define a function $g(x, y)$ with $(x, y) = (L, M)$ as follows:

$$g(x, y) = -\frac{\alpha x^2}{K_l} - \frac{\omega y^2}{K_m} + c_4 x + \omega y.$$

Since the function $g(x, y)$ is concave, it attains a unique maximum value, which is given by:

$$g(x, y) \leq K, \tag{6}$$

■

where $K = \frac{c_4^2 K_l}{4\alpha} + \frac{\omega K_m}{4}$. Based on Inequality (5) and (6), we obtain:

$$\begin{aligned} &\frac{dP_1}{dt} + \varphi P_1 \leq K \\ \Leftrightarrow &\frac{dP_1}{dt} \leq K - \varphi P_1. \end{aligned}$$

Next, we provide the following Equation (7).

$$\frac{dX_1}{dt} = K - \varphi X_1, \quad X_1(0) = P_1(0). \tag{7}$$

The solution to Equation (7) is as follows.

$$X_1(t) = \frac{1}{\varphi}\left(\varphi P_1(0) - K\right) e^{-\varphi t} + \frac{K}{\varphi}.$$

The function $f_1(X_1) = K - \varphi X_1$ is defined, where $K^* = \varphi > 0$. For all $X_{11}, X_{12} \in \Omega$, we obtain:

$$\begin{aligned} |f_1(X_{11}) - f_1(X_{12})| &= |(K^* - \varphi X_{11}) - (K^* - \varphi X_{12})| \\ &= |\varphi X_{11} - \varphi X_{12}| \\ &= \varphi \left| X_{11} - X_{12} \right|. \end{aligned}$$

This indicates that $f_1(X_1)$ satisfies the Lipschitz condition. As a result, by applying the Comparison Theorem [32] and setting $x = X_1(t)$ and $v = P_1(t)$, we obtain:

$$\begin{aligned} &P_1(t) \leq X_1(t) = \frac{1}{\varphi}\left(\varphi P_1(0) - K\right) e^{-\varphi t} + \frac{K}{\varphi} \\ \Leftrightarrow &P_1(t) \leq \frac{1}{\varphi}\left(\varphi P_1(0) - K\right) e^{-\varphi t} + \frac{K}{\varphi} \\ \Rightarrow &\lim_{t\to\infty}(P_1(t)) \leq \lim_{t\to\infty}\left(\frac{1}{\varphi}\left(\varphi P_1(0) - K\right) e^{-\varphi t} + \frac{K}{\varphi}\right) \\ \Leftrightarrow &P_1(t) \leq \frac{K}{\varphi}. \end{aligned} \tag{8}$$

Next, we prove that D is bounded. To demonstrate this, we define the following function:

$$P_2 = L + D. \tag{9}$$

It is important to note that, based on Lemma 3.1, L, C, D, and M are positive. Furthermore, from Function (9), we obtain:

$$\begin{aligned} \frac{dP_2}{dt} =& \frac{dL}{dt} + \frac{dD}{dt} \\ \leq& \alpha L + \beta ML + \theta + (\tau - \sigma)LD - \kappa D. \end{aligned}$$

Because $M \leq c_2 K_m$, $L \leq \frac{K}{\varphi}$, and $\sigma > \tau$, we have:

$$\begin{aligned} \frac{dP_2}{dt} \leq& \frac{\alpha K}{\varphi} + \frac{\beta c_2 K_m K}{\varphi} + \theta - \kappa D + \frac{\kappa K}{\varphi} - \kappa L \\ \leq& c_5 - \kappa(L + D) = c_5 - \kappa P_2, \end{aligned}$$

where $c_5 = \frac{\alpha K}{\varphi} + \frac{\beta c_2 K_m K}{\varphi} + \theta + \frac{\kappa K}{\varphi}$. We assume the equation

$$\frac{dX_2}{dt} = c_5 - \kappa X_2, \quad X_2(0) = P_2(0). \tag{10}$$

Then, the same process is applied to Equation (7), we obtain:

$$\begin{aligned} \lim_{t\to\infty}(P_2(t)) &\leq \lim_{t\to\infty}\left(\frac{1}{\kappa}\left(\kappa P_2(0) - c_5\right) e^{-\kappa t} + \frac{c_5}{\kappa}\right) \\ P_2(t) &\leq \frac{c_5}{\kappa}. \end{aligned} \tag{11}$$

Next, we prove that C is bounded. It is known that $L \leq \frac{K}{\varphi}$ and $D \leq \frac{c_5}{\kappa}$, which implies:

$$\begin{aligned} \frac{dC}{dt} &= \delta LD - \phi LC - \psi MC - \mu C \\ &\leq \delta LD - \mu C \\ &\leq c_6 - \mu C, \end{aligned} \tag{12}$$

where $c_6 = \frac{\delta c_5 K}{\varphi\kappa}$. We assume the equation $\frac{dX_3}{dt} = c_6 - \mu X_3$ with $X_3(0) = C(0)$, and by applying the same procedure as in Equation (7), we obtain:

$$\begin{aligned} &\lim_{t\to\infty}(C(t)) \leq \lim_{t\to\infty}\left(\frac{1}{\mu}\left(\mu C(0) - c_6\right) e^{-\mu t} + \frac{c_6}{\mu}\right) \\ \Leftrightarrow &C(t) \leq \frac{c_6}{\mu}. \end{aligned} \tag{13}$$

Next, we show that the set Ω is positively invariant and bounded. Consider any $(L(0), C(0), D(0), M(0)) \in \Omega$, which implies that $L(0) + C(0) + D(0) + M(0) \leq \bar{c}$, where $\bar{c} = \frac{K}{\varphi} + \frac{c_5}{\kappa} + \frac{c_6}{\mu} + c_2 K_m$. Based on Inequalities (4), (8), (11), and (13), we have:

$$\begin{aligned} &\lim_{t\to\infty}\left(L(t) + C(t) + D(t) + M(t)\right) \\ &\leq \frac{K}{\varphi} + \frac{c_5}{\kappa} + \frac{c_6}{\mu} + c_2 K_m = \bar{c}. \end{aligned}$$

Based on the above discussion, we have shown that Ω is a positively invariant and bounded set. This completes the proof. ■

By straightforward calculation, we find that System (1) has the lung cancer-free equilibrium point.

$$E_0 = \left(0, 0, \frac{\theta\omega}{\eta K_m(\omega - \varphi) + \kappa\omega}, \frac{K_m(\omega - \varphi)}{\omega}\right) \tag{14}$$

and the others equilibria

$$E_{1i} = \left(L_i, C_i, \frac{K_m(\omega - \varphi)}{\omega}, D_i\right), \tag{15}$$

where

$$\begin{aligned} L_i &= \frac{m_1 (D_i)^2 + m_2 D_i + m_3}{m_4 D_i} \\ m_1 &= \gamma q_3 K_l - \sigma q_4 K_l,\ m_2 = bq_4 - \gamma q_2 K_l \\ m_3 &= \gamma q_1 K_l,\ m_4 = \alpha q_4 \\ C_i &= \frac{q_1 + q_2 D_i - q_3 (D_i)^2}{q_4 D_i} \\ q_1 &= \alpha\omega\theta,\ q_2 = b\omega\tau + \eta\varphi K_m - \alpha\omega\eta K_m - \kappa, \\ q_3 &= \omega\tau\sigma K_l,\ q_4 = \omega\tau\gamma K_l + \alpha\omega\varepsilon, \end{aligned}$$

and D_i, $i = 1, 2, 3, 4$, are the solutions of the following quartic equation.

$$p_1 D^4 + p_2 D^3 + p_3 D^2 + p_4 D + p_5 = 0, \tag{16}$$

where

$$\begin{aligned} p_1 &= r_5 q_3^2 - r_2 q_3 q_4 - r_4 q_4^2, \\ p_2 &= r_1 q_4^2 + r_2 q_2 q_4 + r_3 q_3 q_4 - 2 r_5 q_2 q_3, \\ p_3 &= r_2 q_1 q_4 + r_5 (q_2^2 - 2 q_1 q_3) - r_3 q_2 q_4, \\ p_4 &= 2 r_5 q_1 q_2 - r_3 q_1 q_4,\ p_5 = r_5 q_1^2 \\ r_1 &= b\delta\omega,\ r_2 = \phi\omega\sigma K_l - \delta\omega\gamma K_l, \\ r_3 &= b\phi\omega + \alpha\psi K_m(\omega - \varphi) + \mu, \\ r_4 &= \delta\omega\sigma K_l,\ r_5 = \phi\gamma\omega K_l, \end{aligned}$$

IV. Existence and local stability of equilibria

In this section, we demonstrate the existence and stability of the equilibrium points that have been obtained. It is important to note that the lung cancer-free equilibrium point exists when $\omega > \varphi$.

A. Existence of Equiliria

Before demonstrating the existence of the lung cancer-infected equilibrium points E_{1i}, $i = 1, 2, 3, 4$, we first show that the solution of Equation (16) is real and positive. The solution to Equation (16) is given by:

$$D_1 = -\frac{a_1}{4} + \frac{1}{2}(R+T) \tag{17}$$

$$D_2 = -\frac{a_1}{4} + \frac{1}{2}(R-T) \tag{18}$$

$$D_3 = -\frac{a_1}{4} - \frac{1}{2}(R-F) \tag{19}$$

$$D_4 = -\frac{a_1}{4} - \frac{1}{2}(R+F) \tag{20}$$

where

$$a_i = \frac{p_{i+1}}{p_1}, i = 1, 2, 3, 4$$

$$R = \sqrt{\frac{1}{4}a_1^2 - a_2 + y_1} \tag{21}$$

$$T = \begin{cases} \sqrt{\frac{3}{4}a_1^2 - R^2 - 2a_2 + \frac{1}{4}HR^{-1}}, & if R \neq 0 \\ \sqrt{\frac{3}{4}a_1^2 - 2a_2 + 2\sqrt{y_1^2 - 4a_4}}, & if R = 0 \end{cases} \tag{22}$$

$$F = \begin{cases} \sqrt{\frac{3}{4}a_1^2 - R^2 - 2a_2 - \frac{1}{4}HR^{-1}}, & if R \neq 0 \\ \sqrt{\frac{3}{4}a_1^2 - 2a_2 - 2\sqrt{y_1^2 - 4a_4}}, & if R = 0 \end{cases} \tag{23}$$

$$H = 4a_1a_2 - 8a_3 - a_1^3 \tag{24}$$

where y_1 is a real root of cubic equation

$$y^3 - a_2y^2 + (a_1a_3 - 4a_4)y + (4a_2a_4 - a_3^2 - a_1^2a_4) = 0.$$

For a more detailed process in determining the solutions of cubic and quartic equations, refer to [33]. The following presents the existence theorem for the solution of Equation (16) for $R = 0$.

***Theorem** 4.3:* Given Equations (21) to (23), $p_i \in R$ for each $i = 1, 2, 3, 4$ and $p_5 > 0$. If $R = 0$ and

(i) if $p_1 < 0$, $p_2 \leq 0$, and $y_1 < 0$, then D_1 is positive,

(ii) if $p_1 > 0, p_2 \leq 0$, $y_1 > 0$ and $y_1^2 \geq \frac{p_3^2}{p_1^2} - \frac{3p_2^2p_3}{4p_1^3} + \frac{9p_2^4}{64p_1^4} + \frac{4p_5}{p_1}$, then D_2 is positive,

(iii) if $p_1 > 0, p_2 \geq 0$, $y_1 < 0$ and $y_1^2 \geq \frac{4p_5}{p_1}$, then D_3 is positive,

(iv) if $p_1 < 0, p_2 \geq 0$, $y_1 < 0$ and $y_1^2 \leq \frac{p_3^2}{p_1^2} - \frac{3p_2^2p_3}{4p_1^3} + \frac{9p_2^4}{64p_1^4} + \frac{4p_5}{p_1}$, then D_4 is positive,

Proof: We aim to prove that D_1 is positive under the conditions $p_1 < 0$, $p_2 \leq 0$, and $y_1 < 0$. Since $R = 0$, from Equation (21), it follows that $R = 0$ implies $y_1 = -\frac{p_2^2}{4p_1^2} + \frac{p_3}{p_1}$. Therefore, proving that D_1 is positive is equivalent to demonstrating that $-\frac{a_1}{4} + \frac{1}{2}T > 0$. After straightforward calculations, we find that $-\frac{a_1}{4} + \frac{1}{2}T > 0$ holds under the conditions $p_1 < 0$, $p_2 \leq 0$, and $y_1 < 0$. Thus, it is established that D_1 is positive. Similar arguments can be applied to prove conditions (ii), (iii), and (iv). ■

Next, we present a theorem to establish the existence of solutions to Equation (16) for $R > 0$.

***Theorem** 4.4:* Suppose $G = \frac{a_1^2}{2} - a_2 - y_1$, $H = 4a_2a_1 - 8a_3 - a_1^3$, and $R = \sqrt{\frac{a_1^2}{4} - a_2 + y_1}$. If $R > 0$ and

(i) if $G + \frac{H}{4R} > 0$ and $\sqrt{G + \frac{H}{4R}} > \frac{a_1}{2} - R$, then D_1 exists,

(ii) if $G + \frac{H}{4R} > 0$ and $\sqrt{G + \frac{H}{4R}} < R - \frac{a_1}{2}$, then D_2 exists,

(iii) if $G - \frac{H}{4R} > 0$ and $\sqrt{G - \frac{H}{4R}} > \frac{a_1}{2} + R$, then D_3 exists,

(iv) if $-a_1 \geq 0$, $G - \frac{H}{4R} > 0$, and $\sqrt{G - \frac{H}{4R}} < -\left(\frac{a_1}{2} + R\right)$, then D_4 exists.

Proof: Based on Equation (17), demonstrating the existence of D_1 is equivalent to proving that $-\frac{a_1}{4} + \frac{1}{2}(R + T) > 0$. First, it is necessary to establish that T is a real number. According to Equation (22), for $R > 0$, we have $T = \sqrt{\frac{3}{4}a_1^2 - R^2 - 2a_2 + \frac{1}{4}HR^{-1}}$. After performing algebraic manipulations, it can be shown that T is a real number when $G + \frac{H}{4R} > 0$. Subsequently, we demonstrate that D_1 is positive. Further algebraic analysis reveals that $D_1 > 0$ when $\sqrt{G + \frac{H}{4R}} > \frac{a_1}{2} - R$. Therefore, D_1 exists if both conditions $G + \frac{H}{4R} > 0$ and $\sqrt{G + \frac{H}{4R}} > \frac{a_1}{2} - R$ are satisfied. The proofs for conditions (ii), (iii), and (iv) follow a similar rationale. ■

The existence of the lung cancer-infected equilibrium point (15) is established in the following theorem.

***Theorem** 4.5:* Given E_{1i} as the equilibrium points for lung cancer from the system (1) and D_i for $i = 1, 2, 3, 4$ as solutions of Equation (16). If D_i exists and is positive, and if $\left(\gamma q_3 K_l (D_i)^2 + bq_4 D_i\right) > \left(\sigma q_4 K_l (D_i)^2 + \gamma q_2 K_l D_i + \gamma q_1 K_l\right)$ and $q_1 + q_2 D_i > q_3 (D_i)^2$, then the equilibrium points E_{1i} exist for each $i = 1, 2, 3, 4$.

B. Basic Reproduction Number (R_0)

The basic reproduction number of the System (1) can be found using the *next generation matrix* method by having to fulfill some assumptions of the method [34]. Based on the Cancer Differential System, the lung cancer-free equilibrium point is $E_{02} = \left(0, 0, \frac{\theta\omega}{\eta K_m(\omega-\varphi)+\kappa\omega}, \frac{K_m(\omega-\varphi)}{\omega}\right)$. In system (1) there is a disease cell compartment, which is the lung cancer cell compartment (L) and non-lung cancer cell compartments, which are the CD8 + T cell compartment (C), dendritic cells (D) and MSC cells (M). Suppose $\mathbf{x}$ is the disease cell compartment and $\mathbf{y}$ is the non-lung cancer cell compartment, so it can be written as follows.

$$\mathbf{x} = L$$

and

$$\mathbf{y} = \begin{bmatrix} C \\ D \\ M \end{bmatrix}.$$

Then, find the function $\mathcal{F}(\mathbf{x}, \mathbf{y})$ and $\mathcal{V}(\mathbf{x}, \mathbf{y})$ obtained from $\dot{\mathbf{x}} = \mathcal{F}(\mathbf{x}, \mathbf{y}) - \mathcal{V}(x, y)$.

$$\begin{aligned}\dot{\mathbf{x}} =& \frac{dL}{dt} \\ =& \alpha L\left(1 - \frac{L}{K_l}\right) + \beta ML - \gamma LC - \sigma LD \\ =& \left[\alpha L\left(1 - \frac{L}{K_l}\right) + \beta ML\right] - [\gamma LC + \sigma LD] \\ =& \mathcal{F}(\mathbf{x}, \mathbf{y}) - \mathcal{V}(\mathbf{x}, \mathbf{y}).\end{aligned}$$

We obtain $\mathcal{F}(\mathbf{x}, \mathbf{y})$ and $\mathcal{V}(\mathbf{x}, \mathbf{y})$ as follows.

$$\mathcal{F}(x, y) = \alpha L\left(1 - \frac{L}{K_l}\right) + \beta ML \tag{25}$$

and

$$\mathcal{V}(\mathbf{x}, \mathbf{y}) = \gamma LC + \sigma LD. \tag{26}$$

The system (1) satisfies all the assumptions of the *Next Generation Matrix* method. Therefore, the basic reproduction number can be calculated using the *Next Generation Matrix* method. Next, matrices F and V will be constructed, which correspond to the Jacobian matrices of $\mathcal{F}$ and $\mathcal{V}$ at the cancer-free equilibrium point E_0 for lung cancer. Based on Equation (25), the matrix F at the lung cancer-free equilibrium point E_0 is obtained as follows.

$$\begin{aligned}F =& \left[\frac{\partial \mathcal{F}(E_{02})}{\partial x}\right] = \left[\frac{\partial \mathcal{F}(E_{02})}{\partial L}\right] \\ =& \left[\alpha - \frac{2\alpha.0}{K_l} + \beta\left(\frac{K_m(\omega - \varphi)}{\omega}\right)\right] \\ =& \left[\alpha + \left(\frac{\beta K_m(\omega - \varphi)}{\omega}\right)\right].\end{aligned}$$

Then, based on Equation (26), the matrix V at the lung cancer-free equilibrium point E_0 is obtained as follows.

$$\begin{aligned}V =& \left[\frac{\partial \mathcal{V}(E_{02})}{\partial x}\right] = \left[\frac{\partial \mathcal{V}(E_{02})}{\partial L}\right] \\ =& \left[\gamma.0 + \sigma\left(\frac{\theta\omega}{\eta\omega K_m - \eta\varphi K_m + \kappa\omega}\right)\right] \\ =& \left[\left(\frac{\sigma\theta\omega}{\eta\omega K_m - \eta\varphi K_m + \kappa\omega}\right)\right].\end{aligned}$$

Then, we find V^{-1} as follows.

$$V^{-1} = \left[\frac{\eta K_m(\omega - \varphi) + \kappa\omega}{\sigma\theta\omega}\right].$$

Subsequently, the basic reproduction number (R_0) is obtained as follows.

$$\begin{aligned}R_0 =& FV^{-1} \\ =& \frac{\beta\eta K_m^2(\omega - \varphi)^2 + (\alpha\eta + \beta\kappa)\omega K_m(\omega - \varphi) + \alpha\kappa\omega^2}{\omega^2\sigma\theta}.\end{aligned}$$

C. The Stability of Equilibria

In this section, the local stability of the equilibrium points is analyzed by examining the eigenvalues of the Jacobian matrix associated with System (1). The stability of each equilibrium point is determined by the sign of the real parts of its eigenvalues. The Jacobian matrix for System (1) is presented as follows:

$$\begin{bmatrix} A_{11} & A_{12} & A_{13} & A_{14} \\ A_{21} & A_{22} & A_{23} & A_{24} \\ A_{31} & A_{32} & A_{33} & A_{34} \\ 0 & 0 & 0 & A_{44} \end{bmatrix} \tag{27}$$

where

$$\begin{aligned}&A_{11} = \alpha - \frac{2\alpha L}{K_l} + \beta M - \gamma C - \sigma D,\ A_{12} = -\gamma L, \\ &A_{13} = -\sigma L,\ A_{14} = \beta L,\ A_{21} = \delta D \\ &A_{22} = -\phi L - \psi M - \mu,\ A_{23} = \delta L, \\ &A_{24} = -\psi C,\ A_{31} = \tau D \\ &A_{32} = -\varepsilon D,\ A_{33} = \tau L - \varepsilon C - \eta M - \kappa, \\ &A_{44} = \omega - \frac{2\omega M}{K_m} - \varphi.\end{aligned}$$

To evaluate the stability of the lung cancer-free equilibrium point, we use the basic reproduction number (R_0) obtained in the previous section. A theorem is presented to establish the stability of the lung cancer-free equilibrium point.

***Theorem** 4.6:* If $R_0 < 1$, then the equilibrium point $E_0 = \left(0, 0, \frac{\theta\omega}{\eta K_m(\omega - \varphi) + \kappa\omega}, \frac{K_m(\omega - \varphi)}{\omega}\right)$ is locally asymptotically stable.

Proof: The eigenvalues of the Jacobian matrix of the System (1) at the equilibrium point E_0 are

$$\lambda_1 = -\frac{\sigma\theta\omega}{\eta K_m(\omega - \varphi) + \kappa\omega} + \frac{\beta K_m(\omega - \varphi)}{\omega} + \alpha \tag{28}$$

$$\lambda_2 = -\frac{K_m(\omega - \varphi)\psi}{\omega} - \mu \tag{29}$$

$$\lambda_3 = -\frac{K_m(\omega - \varphi)\eta}{\omega} - \kappa \tag{30}$$

$$\lambda_4 = -\omega + \varphi. \tag{31}$$

Since each parameter in System (1) is positive and $\omega > \varphi$, the eigenvalues λ_2, λ_3, and λ_4 are negative. The equilibrium point E_0 is locally asymptotically stable if λ_1 is negative. Given that $R_0 < 1$, we have:

$$\begin{aligned}&\left[\alpha + \left(\frac{\beta K_m(\omega - \varphi)}{\omega}\right)\right]\left[\frac{\eta K_m(\omega - \varphi) + \kappa\omega}{\sigma\theta\omega}\right] < 1 \\ \Leftrightarrow &\left[\alpha + \left(\frac{\beta K_m(\omega - \varphi)}{\omega}\right)\right] < \left[\frac{\sigma\theta\omega}{\eta K_m(\omega - \varphi) + \kappa\omega}\right] \\ \Leftrightarrow &\left[\alpha + \left(\frac{\beta K_m(\omega - \varphi)}{\omega}\right)\right] - \left[\frac{\sigma\theta\omega}{\eta K_m(\omega - \varphi) + \kappa\omega}\right] < 0 \\ \Leftrightarrow &\lambda_1 < 0.\end{aligned}$$

Thus, the equilibrium point E_0 is locally asymptotically stable when $R_0 < 1$. ■

Next, we perform stability analysis for the equilibrium points E_{1i}, where $i = 1, 2, 3, 4$. First, we define the following

variables:

$$C_{11} = \alpha - \frac{2\alpha L_i}{K_l} + \frac{\beta K_m(\omega-\varphi)}{\omega} - \gamma C_i - \sigma D_i,$$
$$C_{12} = -\gamma L_i,\ C_{13} = -\sigma L_i, C_{14} = \beta L_i,\ C_{21} = \delta D_i,$$
$$C_{22} = -\phi L_i - \frac{\psi K_m(\omega-\varphi)}{\omega} - \mu, C_{23} = \delta L_i,$$
$$C_{24} = -\psi C_i,\ C_{31} = \tau D_i,\ C_{32} = -\varepsilon D_i,$$
$$C_{33} = \tau L_i - \varepsilon C_i - \frac{\eta K_m(\omega-\varphi)}{\omega} - \kappa,\ C_{44} = -\omega + \varphi.$$

The characteristic equation of the system (1) corresponding to the equilibrium point $E_{1i} = \left(L_i, C_i, D_i, \frac{K_m(\omega-\varphi)}{\omega}\right)$ is as follows.

$$\lambda^4 + h_1\lambda^3 + h_2\lambda^2 + h_3\lambda + h_4 = 0, \tag{32}$$

where

$$\begin{aligned}
h_1 =& -C_{11} - C_{22} - C_{33} - C_{44}\\
h_2 =& C_{11}C_{44} + C_{22}C_{44} + C_{33}C_{44} + C_{11}C_{22} + C_{11}C_{33}\\
&+ C_{22}C_{33} - C_{32}C_{23} - C_{12}C_{21} - C_{13}C_{31}\\
h_3 =& -C_{11}C_{22}C_{44} - C_{11}C_{33}C_{44} + C_{32}C_{23}C_{44}\\
&+ C_{12}C_{21}C_{44} + C_{13}C_{31}C_{44} - C_{11}C_{22}C_{33}\\
&+ C_{11}C_{32}C_{23} + C_{12}C_{21}C_{33} - C_{12}C_{31}C_{23}\\
&- C_{13}C_{21}C_{32} + C_{13}C_{31}C_{22}\\
h_4 =& C_{11}C_{22}C_{33}C_{44} - C_{11}C_{32}C_{23}C_{44} - C_{12}C_{21}C_{33}C_{44}\\
&+ C_{12}C_{31}C_{23}C_{44} + C_{13}C_{21}C_{32}C_{44} - C_{13}C_{31}C_{22}C_{44}.
\end{aligned}$$

According to the Routh-Hurwitz criterion, all solutions of the characteristic equation (32) are negative if the following conditions are satisfied: $h_j > 0$, for $j = 1, 2, 3, 4$, $h_1h_2 - h_3 > 0$, and $h_3(h_1h_2 - h_3) - h_1^2h_4 > 0$. Based on these conditions, the stability criteria for the equilibrium point E_{1i} are given in Theorem 4.7.

***Theorem** 4.7:* If the equilibrium point E_{1i} exists and if $h_1 > 0$, $h_4 > 0$, $h_1h_2 - h_3 > 0$, and $h_3(h_1h_2 - h_3) - h_1^2h_4 > 0$, then the equilibrium point E_{1i} is locally asymptotically stable.

V. SIMULATION RESULTS

In this section, we present numerical simulations to illustrate the stability and existence of the equilibrium points, as analyzed in the previous section. The parameter values employed in the simulations are provided in Table I. These parameters were sourced from various references, including [31], [30], [35], [36], and [37].

The numerical simulations to be conducted will include a sensitivity analysis, simulations of the cancer-free equilibrium point, simulations of the lung cancer equilibrium point, and simulations of R_0 as a function of the parameters β and θ.

A. Sensitivity Analysis

In this subsection, we perform a sensitivity index analysis of the basic reproduction number (R_0) with respect to the parameters employed in the model. The objective of this analysis is to identify the parameters that significantly influence variations in the value of R_0. The formula used for the sensitivity analysis is provided in [38].

TABLE I
MATHEMATICAL MODEL PARAMETERS

Parameter	Values	Unit	Description
α	0.23	day^{-1}	[31]
K_l	1.02×10^9	$cells.mm^{-3}.day^{-1}$	[30]
β	10^{-8}	$cells^{-1}.mm^3.day^{-1}$	Estimated
γ	10^{-7}	$cells^{-1}.mm^3.day^{-1}$	[30]
σ	1.1×10^{-5}	$cells^{-1}.mm^3.day^{-1}$	Estimated
δ	0.01	$cells^{-1}.mm^3.day^{-1}$	[30]
ϕ	3.40×10^{-10}	$cells^{-1}.mm^3.day^{-1}$	[30]
ψ	10^{-8}	$cells^{-1}.mm^3.day^{-1}$	Estimated
μ	2×10^{-2}	day^{-1}	[30]
θ	5.8×10^2	$cells.mm^{-3}.day^{-1}$	[30]
τ	10^{-7}	$cells^{-1}mm^3day^{-1}$	[30]
ε	10^{-8}	$cells^{-1}.mm^3.day^{-1}$	[30]
η	10^{-6}	$cells^{-1}.mm^3.day^{-1}$	Estimated
κ	2.4×10^{-2}	day^{-1}	[30]
ω	0.77	day^{-1}	[35]
K_m	762.922	$cells.mm^{-3}.day^{-1}$	[36]
φ	0.18	day^{-1}	[37]

$$\Upsilon_p^v = \frac{\partial v}{\partial p} \times \frac{p}{v},$$

where v being the variable to be analyzed and p the parameter. Based on the analysis results using the formula above, the sensitivity indices of R_0 with respect to several parameters can be either positive or negative. These sensitivity values are presented in Table II below.

TABLE II
THE SENSITIVITY INDICES OF R_0

Parameter	Sensitivity Index
α	0.9999745837
β	0.2541573×10^{-4}
η	0.2435143×10^{-3}
K_m	0.2689299×10^{-3}
κ	0.9997564860
φ	$-0.8204644 \times 10^{-4}$
σ	-1
θ	-1
ω	0.8204683×10^{-4}

The sensitivity indices with positive values include the parameters α, β, η, K_m, κ, and ω. This indicates that an increase in any of these parameters, while holding the others constant, results in an increase in R_0, thereby promoting higher endemicity of lung cancer cells. Conversely, the parameters with negative sensitivity indices are φ, σ, and θ. An increase in any of these parameters, while the others remain constant, leads to a decrease in R_0, which corresponds to a reduction in the endemicity of lung cancer cells. As shown in Table II, the parameters σ and θ play a particularly significant role in reducing the value of R_0. From a medical perspective, this underscores the critical importance of dendritic cells in the treatment of lung cancer.

B. Numerical Simulation of the Lung Cancer-Free Equilibrium Point

In the case of the lung cancer-free equilibrium point, the parameter values used are those presented in Table I, which satisfy the conditions specified in Theorem 4.6. With these parameter values, the conditions in Theorem 4.6 are satisfied, resulting in $R_0 = 0.8863003657 < 1$. The system described

by equation (1) has a lung cancer-free equilibrium point at $(0, 0, 23592.02721, 584.5765974)$.

Figure 2 illustrates the behavior of the system using the initial values $(100, 0, 1000, 100)$. The concentrations of lung cancer cells, CD8+ T cells, dendritic cells, and MSCs converge to the lung cancer-free equilibrium point as $t \to \infty$. Medically, this indicates that, over time, the lung cancer cells will be eliminated. Additionally, Figure 2 shows that the CD8+ T cells also approach zero. From a medical perspective, this occurs because CD8+ T cells identic are active only in the presence of lung cancer cells.

C. Numerical Simulation of Lung Cancer-infected Equilibrium Points in Lung Cancer

Case (i) There is one equilibrium point, E_{1i}, in this case. The parameters are chosen to satisfy the conditions in Theorem 4.4 and Theorem 4.5. The selected parameter values are $\beta = 10^{-6}$, $\sigma = 10^{-6}$, $\phi = 3 \times 10^{-8}$, $\theta = 2 \times 10^{2}$, $\tau = 5 \times 10^{-7}$, $\varepsilon = 10^{-7}$, and $\eta = 10^{-8}$, while the other parameters not mentioned are taken from Table I. With these parameter values, the conditions in Theorem 4.4 are satisfied, yielding four positive D values: $D_1 = 2.53856 \times 10^{5}$, $D_2 = 797.02$, $D_3 = 6.577208$, and $D_4 = 0.252652$. Among these, only D_2 satisfies the conditions in Theorem 4.5. Thus, the equilibrium point is $E_{12} = (5818.16, 2.29786247 \times 10^{6}, 797.02, 584.58)$. Furthermore, at the equilibrium point E_{12}, $h_1 = 0.8611173479 > 0$, $h_4 = 0.6923514607 \times 10^{-3} > 0$, $h_1 h_2 - h_3 = 0.1434460188 > 0$ and $h_3(h_1 h_2 - h_3) - h_1^2 h_4 = 0.4400738769 \times 10^{-3} > 0$ are obtained so that the conditions in Theorem 4.7 are fulfilled. Thus, the equilibrium point E_{12} is locally asymptotically stable as shown in Figure 3.

Figure 3 illustrates the dynamics of the concentrations of lung cancer cells, CD8+ T cells, dendritic cells, and MSCs. With initial values of $(1000, 100, 10, 100)$, the figure shows that the concentration of each cell type converges to the equilibrium point E_{12} over time. Medically, this suggests that lung cancer cells persist in the body. This condition is further supported by the presence of CD8+ T cells, which remain active. It is well-known that CD8+ T cells are activated in response to disturbances, such as the presence of lung cancer cells. The asymptotically stable equilibrium point indicates that, over time, the lung cancer cells cease to spread or their progression does not worsen, suggesting that the growth of lung cancer cells can be controlled.

Case (ii) There are two equilibrium points, E_{1i}. The parameter values are selected to satisfy the conditions in Theorem 4.4 and Theorem 4.5. The chosen parameters are $\beta = 10^{-6}$, $\gamma = 10^{-9}$, $\sigma = 10^{-4}$, $\phi = 3 \times 10^{-10}$, $\psi = 10^{-5}$, $\theta = 2 \times 10^{2}$, $\varepsilon = 10^{-7}$, and $\eta = 10^{-8}$. For parameters not explicitly mentioned, the values listed in Table I are used. With these parameter values, the conditions in Theorem 4.4 $(i)-(iii)$ are satisfied. As a result, three positive solutions are obtained from the quartic Equation (16): $D_1 = 2299.540282$, $D_2 = 14.099074$, and $D_3 = 4.369612452$. Among these, D_1 and D_2 satisfy the conditions in Theorem 4.5, leading to the identification of two equilibrium points.

$E_{11} = (708.5339, 6.303886 \times 10^{5}, 2299.540282, 584, 5766)$,
$E_{12} = (7.1450135 \times 10^{7}, 2.13063364 \times 10^{8}, 14.099, 584.577)$.

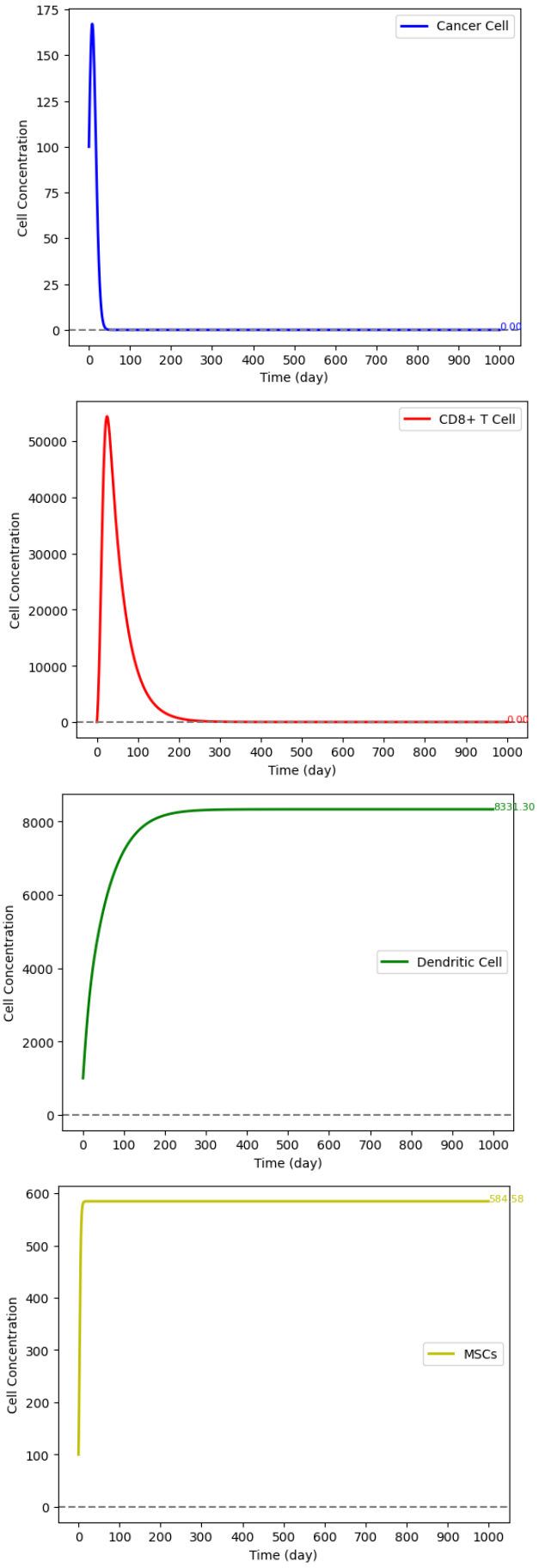

Fig. 2. Cell Concentrations at the Lung Cancer-Free Equilibrium Point

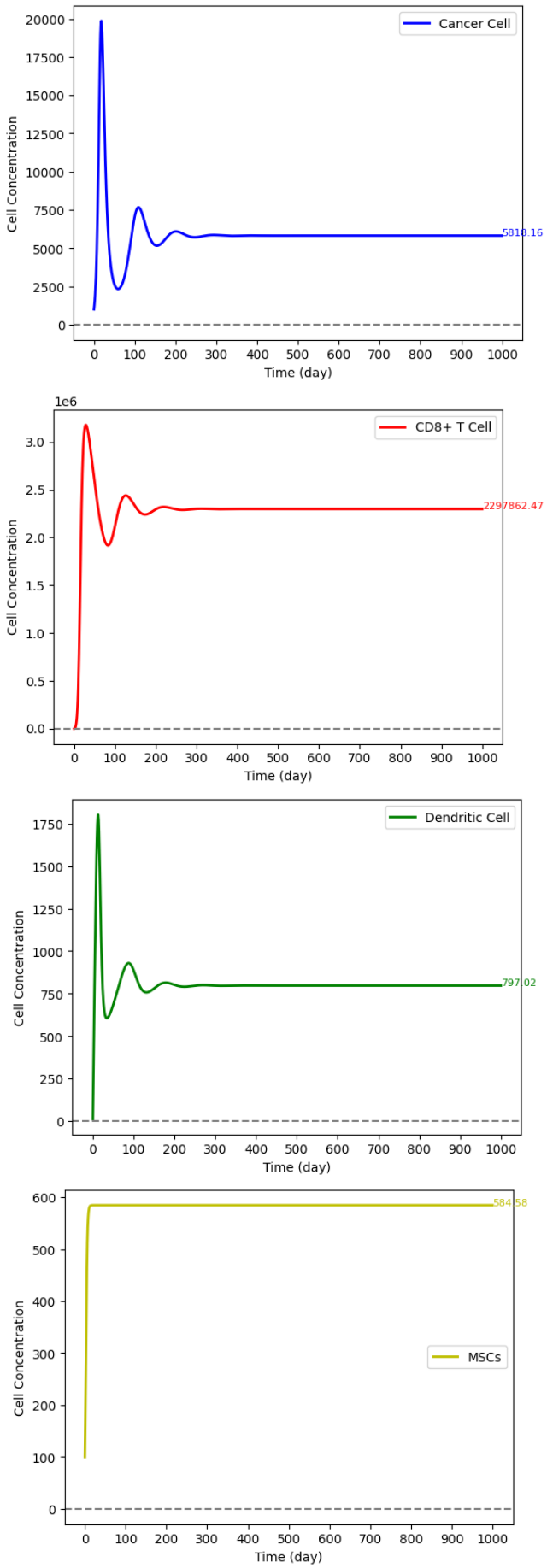

Fig. 3. Cell Concentrations at the Lung Cancer-infected Equilibrium Point

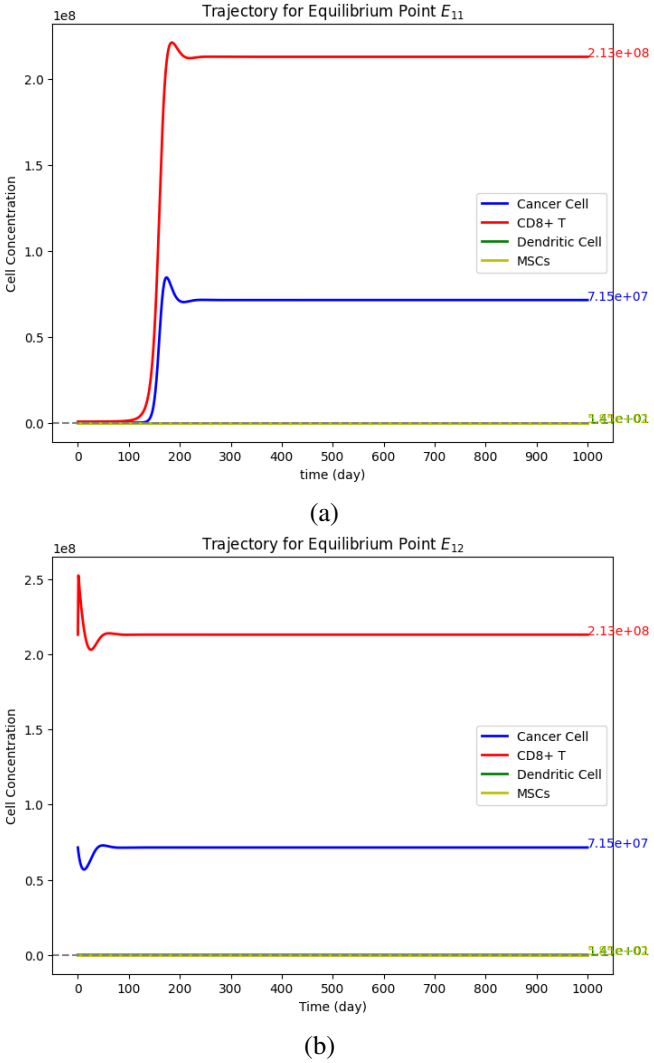

Fig. 4. Cell Concentration at the Equilibrium Point of Lung Cancer Infection

At the equilibrium point E_{11}, it is determined that $h_4 = -0.2199746117 \times 10^{-3} < 0$, which does not satisfy the conditions in Theorem 4.7. Furthermore, calculations performed using MAPLE software reveal that the Jacobian matrix at E_{11} has one positive eigenvalue and three negative eigenvalues, indicating that the equilibrium point E_{11} is unstable. Conversely, at the equilibrium point E_{12}, the following conditions are satisfied: $h_1 = 14.83872085 > 0$, $h_4 = 0.1421721317 > 0$, $h_1h_2 - h_3 = 152.3648957 > 0$, and $h_3(h_1h_2 - h_3) - h_1^2h_4 = 118.3942590 > 0$. These results confirm that the conditions in Theorem 4.7 are met. Therefore, the equilibrium point E_{12} is locally asymptotically stable. The trajectory plots for the equilibrium points E_{11} and E_{12} are presented in Figure 4. In Figure 4 (a), it is observed that with initial values of $(808.5339736, 6.302891368 \times 10^5, 2399.540277, 584.5765974)$, which are sufficiently close to the equilibrium point E_{11}, the trajectory does not converge to E_{11}. This behavior indicates that E_{11} is unstable. In contrast, Figure 4 (b) shows that with initial values of $(7.145113516 \times 10^7, 2.130643641 \times 10^8, 1014.099074, 594.5765974)$, the trajectory converges to the equilibrium point E_{12}, indicating that E_{12} is locally asymptotically stable. Medically, the instability of the equi-

librium point suggests that the growth of lung cancer cells is likely to be uncontrolled, preventing the cessation of their spread. This implies a high risk of increased lung cancer cell proliferation over time.

D. Simulation of R_0 with Respect to the Parameter β

The sensitivity of R_0 with respect to β is used to assess the influence of MSC cells on the growth of lung cancer cells. Using the parameter values listed in Table I, the function R_0 with respect to the parameter β is obtained as follows.

$$Ro = 2252.596886\beta + 0.8862778398.$$

Below is the graph of the function Ro with respect to the parameter β.

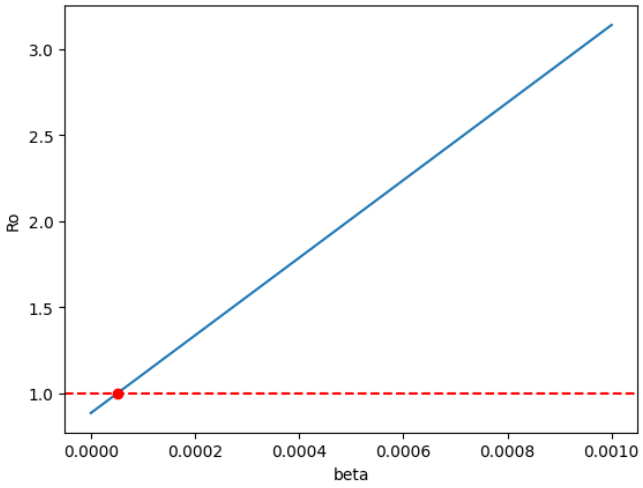

Fig. 5. Simulation of Ro with respect to the parameter β

Based on Figure 5, it is observed that R_0 exceeds one when $\beta > 0.5048491406 \times 10^{-4}$, and falls below one when $\beta < 0.5048491406 \times 10^{-4}$. Since β is the contribution rate of MSCs cells to the growth of lung cancer cells, medically it suggests that if each MSCs cell increases the lung cancer volume by more than $0.5048491406 \times 10^{-4}$ mm^3 day^{-1}, lung cancer will progress and persist in the body.

E. Simulation of Ro with Respect to The parameter θ

The sensitivity of R_0 with respect to θ is employed to evaluate the impact of dendritic cells on lung cancer cell proliferation. Using the parameter values from Table I, the function R_0 with respect to the parameter θ is given by the following expression.

$$Ro = \frac{514.0542121}{\theta}.$$

Figure 6 is the graph of the function Ro with respect to the parameter θ.

Based on Figure 6, it is observed that R_0 exceeds one when $\theta < 514.0542121$, and falls below one when $\theta > 514.0542121$. Since θ is the production rate of dendritic cells, medically it shows that if the production rate of dendritic cells is more than 514.0542121 cells/mm^3 per day and other parameters have fixed values according to Table I then the growth of lung cancer can be prevented.

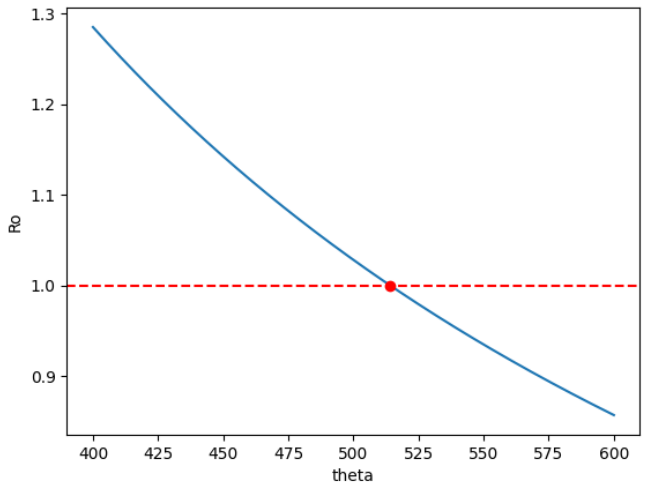

Fig. 6. Simulation of Ro with respect to the parameter θ"

VI. Conclusion

The mathematical model (1) provides a good representation of the dynamics of lung cancer growth, considering the response of innate immune cells such as CD8+ T cells and dendritic cells, as well as the role of MSCs. Based on this model, a lung cancer-free equilibrium point E_0 and four non-cancer-free equilibrium points E_{1i} for $i = 1, 2, 3, 4$ are obtained. The lung cancer-free equilibrium point is locally asymptotically stable when the basic reproduction number $R_0 < 1$. Conversely, the lung cancer-infected equilibrium points are asymptotically stable when the conditions in Theorem 4.7 are satisfied.

Based on the sensitivity analysis, the parameters that have the most significant influence in reducing the risk of lung cancer cell growth are the parameters σ and θ. The parameter σ represents the mortality rate of lung cancer cells due to interaction with dendritic cells, while the parameter θ represents the production rate of dendritic cells, which is assumed to be constant. This highlights the important role of dendritic cells in the process of managing lung cancer. On the other hand, one of the parameters that most significantly accelerates lung cancer growth is the parameter β, which represents the interaction rate between MSCs and lung cancer cells.

Therefore, the analysis conducted in this study suggests that efforts to prevent the growth of lung cancer cells can be made by increasing the production of dendritic cells. Additionally, another approach that can be taken is to prevent the recruitment of MSCs into lung cancer cells.

Based on the explanation above, the parameters that play a significant role in reducing the value of R_0 are the parameters σ and θ. The parameter σ represents the mortality rate of lung cancer cells due to interaction with dendritic cells, while the parameter θ represents the production rate of dendritic cells, which is assumed to be constant. This highlights the crucial role of dendritic cells in the management of lung cancer.

Therefore, it can be concluded that efforts to prevent the growth of lung cancer cells can be undertaken by increasing the production of dendritic cells. This is because, based on medical evidence and the results of the analysis conducted in this study, dendritic cells have been found to be effective in inhibiting the growth of lung cancer cells. Additionally,

another measure that can be taken is to prevent the recruitment of MSCs (Mesenchymal Stem Cells) into lung cancer cells.

Furthermore, numerical simulations of the lung cancer-free equilibrium point show that when it is asymptotically stable, lung cancer cells will disappear over time. Conversely, when the non-cancer-free equilibrium points are asymptotically stable, lung cancer cells will persist in the body.

ACKNOWLEDGMENT

We would like to thank our Supervisor for providing guidance and direction throughout the preparation of this article.

REFERENCES

[1] L. Zhang, Y. Li, C.-Y. Guan, S. Tian, X.-D. Lv, J.-H. Li, X. Ma, and H.-F. Xia, "Therapeutic effect of human umbilical cord-derived mesenchymal stem cells on injured rat endometrium during its chronic phase," *Stem cell research & therapy*, vol. 9, pp. 1–15, 2018.

[2] C. R. Lindsay, E. C. Shaw, D. A. Moore, D. Rassl, M. Jamal-Hanjani, N. Steele, S. Naheed, C. Dick, F. Taylor, H. Adderley *et al.*, "Large cell neuroendocrine lung carcinoma: consensus statement from the british thoracic oncology group and the association of pulmonary pathologists," *British journal of cancer*, vol. 125, no. 9, pp. 1210–1216, 2021.

[3] A. S. Jain, A. Prasad, S. Pradeep, C. Dharmashekar, R. R. Achar, E. Silina, V. Stupin, R. G. Amachawadi, S. K. Prasad, R. Pruthvish *et al.*, "Everything old is new again: drug repurposing approach for non-small cell lung cancer targeting mapk signaling pathway," *Frontiers in oncology*, vol. 11, p. 741326, 2021.

[4] D. Pandey, P. Ramanathan, R. Pandey, and K. Prabhash, "Mediastinal staging for non-small cell lung cancer revisited. it is being done under aegis of icon and lung cancer consortium asia," *Indian Journal of Cancer*, vol. 54, no. 1, pp. 68–72, 2017.

[5] D. E. Kelley, M. H. Boynton, S. M. Noar, J. C. Morgan, J. R. Mendel, K. M. Ribisl, I. Stepanov, L. A. Nylander-French, and N. T. Brewer, "Effective message elements for disclosures about chemicals in cigarette smoke," *Nicotine and Tobacco Research*, vol. 20, no. 9, pp. 1047–1054, 2018.

[6] Y.-J. Jiang, C.-C. Chao, A.-C. Chang, P.-C. Chen, F.-J. Cheng, J.-F. Liu, P.-I. Liu, C.-L. Huang, J.-H. Guo, W.-C. Huang *et al.*, "Cigarette smoke-promoted increases in osteopontin expression attract mesenchymal stem cell recruitment and facilitate lung cancer metastasis," *Journal of Advanced Research*, vol. 41, pp. 77–87, 2022.

[7] X. Fu, G. Liu, A. Halim, Y. Ju, Q. Luo, and G. Song, "Mesenchymal stem cell migration and tissue repair," *Cells*, vol. 8, no. 8, p. 784, 2019.

[8] H. Lin, J. Sohn, H. Shen, M. T. Langhans, and R. S. Tuan, "Bone marrow mesenchymal stem cells: Aging and tissue engineering applications to enhance bone healing," *Biomaterials*, vol. 203, pp. 96–110, 2019.

[9] S. A. Wexler, C. Donaldson, P. Denning-Kendall, C. Rice, B. Bradley, and J. M. Hows, "Adult bone marrow is a rich source of human mesenchymal 'stem'cells but umbilical cord and mobilized adult blood are not," *British journal of haematology*, vol. 121, no. 2, pp. 368–374, 2003.

[10] E. H. Park, H.-s. Lim, S. Lee, K. Roh, K.-W. Seo, K.-S. Kang, and K. Shin, "Intravenous infusion of umbilical cord blood-derived mesenchymal stem cells in rheumatoid arthritis: a phase ia clinical trial," *Stem cells translational medicine*, vol. 7, no. 9, pp. 636–642, 2018.

[11] J.-Y. Li, K.-K. Ren, W.-J. Zhang, L. Xiao, H.-Y. Wu, Q.-Y. Liu, T. Ding, X.-C. Zhang, W.-J. Nie, Y. Ke *et al.*, "Human amniotic mesenchymal stem cells and their paracrine factors promote wound healing by inhibiting heat stress-induced skin cell apoptosis and enhancing their proliferation through activating pi3k/akt signaling pathway," *Stem cell research & therapy*, vol. 10, pp. 1–17, 2019.

[12] A. Bier, P. Berenstein, N. Kronfeld, D. Morgoulis, A. Ziv-Av, H. Goldstein, G. Kazimirsky, S. Cazacu, R. Meir, R. Popovtzer *et al.*, "Placenta-derived mesenchymal stromal cells and their exosomes exert therapeutic effects in duchenne muscular dystrophy," *Biomaterials*, vol. 174, pp. 67–78, 2018.

[13] A. L. F. Longhini, T. E. Salazar, C. Vieira, T. Trinh, Y. Duan, L. M. Pay, S. Li Calzi, M. Losh, N. A. Johnston, H. Xie *et al.*, "Peripheral blood-derived mesenchymal stem cells demonstrate immunomodulatory potential for therapeutic use in horses," *PLoS One*, vol. 14, no. 3, p. e0212642, 2019.

[14] W. M. Jackson, L. J. Nesti, and R. S. Tuan, "Potential therapeutic applications of muscle-derived mesenchymal stem and progenitor cells," *Expert opinion on biological therapy*, vol. 10, no. 4, pp. 505–517, 2010.

[15] T. Cheng, Y. Feng, X. Chen, J. Zhou, and Y. Song, "Lung-resident mesenchymal stem cells regulated the inflammatory responses in innate and adaptive immune cells through hvem-btla pathway during ards," *Experimental Cell Research*, vol. 395, no. 1, p. 112155, 2020.

[16] G. Fregni, M. Quinodoz, E. Möller, J. Vuille, S. Galland, C. Fusco, P. Martin, I. Letovanec, P. Provero, C. Rivolta *et al.*, "Reciprocal modulation of mesenchymal stem cells and tumor cells promotes lung cancer metastasis," *EBioMedicine*, vol. 29, pp. 128–145, 2018.

[17] N. Li and J. Hua, "Interactions between mesenchymal stem cells and the immune system," *Cellular and Molecular Life Sciences*, vol. 74, pp. 2345–2360, 2017.

[18] S. K. Wculek, F. J. Cueto, A. M. Mujal, I. Melero, M. F. Krummel, and D. Sancho, "Dendritic cells in cancer immunology and immunotherapy," *Nature Reviews Immunology*, vol. 20, no. 1, pp. 7–24, 2020.

[19] R. Ruez, J. Dubrot, A. Zoso, M. Bacchetta, F. Molica, S. Hugues, B. R. Kwak, and M. Chanson, "Dendritic cell migration toward ccl21 gradient requires functional cx43," *Frontiers in physiology*, vol. 9, p. 288, 2018.

[20] K. Gwin, J. J. Dolence, M. B. Shapiro, and K. L. Medina, "Differential requirement for hoxa9 in the development and differentiation of b, nk, and dc-lineage cells from flt3+ multipotential progenitors," *BMC immunology*, vol. 14, pp. 1–9, 2013.

[21] D. Benteyn, C. Heirman, A. Bonehill, K. Thielemans, and K. Breckpot, "mrna-based dendritic cell vaccines," *Expert review of vaccines*, vol. 14, no. 2, pp. 161–176, 2015.

[22] C. E. Bryant, S. Sutherland, B. Kong, M. S. Papadimitrious, P. D. Fromm, and D. N. Hart, "Dendritic cells as cancer therapeutics," in *Seminars in Cell & Developmental Biology*, vol. 86. Elsevier, 2019, pp. 77–88.

[23] P. Zhao, X. Bu, X. Wei, W. Sun, X. Xie, C. Li, Q. Guo, D. Zhu, X. Wei, and D. Gao, "Dendritic cell immunotherapy combined with cytokine-induced killer cells promotes skewing toward th2 cytokine profile in patients with metastatic non-small cell lung cancer," *International immunopharmacology*, vol. 25, no. 2, pp. 450–456, 2015.

[24] D. Stevens, J. Ingels, S. Van Lint, B. Vandekerckhove, and K. Vermaelen, "Dendritic cell-based immunotherapy in lung cancer," *Frontiers in immunology*, vol. 11, p. 620374, 2021.

[25] N. Larmonier, J. Fraszczak, D. Lakomy, B. Bonnotte, and E. Katsanis, "Killer dendritic cells and their potential for cancer immunotherapy," *Cancer Immunology, Immunotherapy*, vol. 59, pp. 1–11, 2010.

[26] H. Raskov, A. Orhan, J. P. Christensen, and I. Gögenur, "Cytotoxic cd8+ t cells in cancer and cancer immunotherapy," *British journal of cancer*, vol. 124, no. 2, pp. 359–367, 2021.

[27] C. Fu and A. Jiang, "Dendritic cells and cd8 t cell immunity in tumor microenvironment," *Frontiers in immunology*, vol. 9, p. 3059, 2018.

[28] J. Wu, Y. Zhu, M. Luo, and L. Li, "Comprehensive analysis of pyroptosis-related genes and tumor microenvironment infiltration characterization in breast cancer," *Frontiers in Immunology*, vol. 12, p. 748221, 2021.

[29] W. H. Fridman, F. Pagès, C. Sautès-Fridman, and J. Galon, "The immune contexture in human tumours: impact on clinical outcome," *Nature Reviews Cancer*, vol. 12, no. 4, pp. 298–306, 2012.

[30] M. A. Ullah and U. K. Mallick, "Mathematical modeling and analysis on the effects of surgery and chemotherapy on lung cancer," *Journal of Applied Mathematics*, vol. 2023, no. 1, p. 4201373, 2023.

[31] R. Eftimie and C. Barelle, "Mathematical investigation of innate immune responses to lung cancer: The role of macrophages with mixed phenotypes," *Journal of Theoretical Biology*, vol. 524, p. 110739, 2021.

[32] Z. Qu, *Cooperative control of dynamical systems: applications to autonomous vehicles*. Springer Science & Business Media, 2009.

[33] Y.-B. Jia, *Roots of Polynomials*, 2022.

[34] C. Castillo-Chavez and F. Brauer, *Mathematical Models in Population Biology and Epidemiology*, ser. Texts in Applied Mathematics. New York: Springer, 2012, vol. 40.

[35] L. Wadkin, S. Orozco-Fuentes, I. Neganova, M. Lako, A. Shukurov, and N. Parker, "The recent advances in the mathematical modelling of human pluripotent stem cells," *SN Applied Sciences*, vol. 2, no. 2, p. 276, 2020.

[36] M. A. Tabatabai, Z. Bursac, W. M. Eby, and K. P. Singh, "Mathematical modeling of stem cell proliferation," *Medical & biological engineering & computing*, vol. 49, pp. 253–262, 2011.

[37] A. Yazdani, F. Bahrami, A. Pourgholaminejad, and R. Moghadasali, "A biological and a mathematical model of sle treated by mesenchymal stem cells covering all the stages of the disease," *Theory in Biosciences*, vol. 142, no. 2, pp. 167–179, 2023.

[38] S. Olaniyi, M. A. Lawal, and O. S. Obabiyi, "Stability and sensitivity analysis of a deterministic epidemiological model with pseudo-recovery," *IAENG International Journal of Applied Mathematics*, vol. 46, no. 2, pp. 160–167, 2016.